Anomalous Sorption Kinetics in the Methanol Vapor–Poly(methyl methacrylate) System

V. Dimos, M. Sanopoulou

Institute of Physical Chemistry, National Center for Scientific Research "Demokritos", GR-15310 Agia Paraskevi, Athens, Greece

Received 16 November 2004; accepted 17 December 2004
DOI 10.1002/app.21860
Published online in Wiley InterScience (www.interscience.wiley.com).

ABSTRACT: The non-Fickian sorption kinetics of methanol vapor in poly(methyl methacrylate) films 8 and 51 μm thick at 25°C are presented. The behavior of the system was studied in series of interval and integral absorption runs. The relevant diffusion coefficient and viscous relaxation processes were studied separately by kinetic analysis of the first and second stages of sorption kinetic curves. The sorption isotherm concaved upward at high activities, this being typical of Flory–Huggins behavior, whereas it exhibited a convex-upward curvature at low methanol vapor activities, this indicating sorption in the excess free volume of the polymer matrix. After excess free-volume fill-up, the concentration dependence of the diffusion coefficient was found to be well represented by the free-volume theory of Vrentas and Duda. Relaxation frequencies calculated from the second stage of two-stage curves exhibited a weak dependence on the concentration. Integral sorption experiments indicated that the system exhibited nearly case II kinetics at high methanol vapor activities. © 2005 Wiley Periodicals, Inc. J Appl Polym Sci 97: 1184–1195, 2005

Key words: diffusion; relaxation; swelling

INTRODUCTION

The drying of polymer membranes, the dry spinning of fibers, the coating of substrates with polymers, and many other industrial processes depend on non-Fickian diffusion of organic solvents in polymers. This also applies to polymer industry product design, including food packaging materials, separation membranes, and controlled-drug-release systems. Clearly, an in-depth understanding of the anomalous sorption process would offer a great advantage to the polymer industry.

Sorption kinetic experiments are the most common way of studying the diffusion of various vapor or gas penetrants in polymeric materials. Such experiments are carried out by immerging a thin polymer film of thickness l in a given penetrant atmosphere, at constant pressure (activity) and temperature. To obtain an absorption (desorption) curve, after thermodynamic equilibrium has been achieved, one must raise (lower) the vapor pressure of the penetrant from its initial value (p_i) to a final constant value (p_f) and record the mass gain (loss) of the film [instant sorbed mass (Q_t)] as a function of time (t) until a new equilibrium is achieved (at $t \to \infty$). Fickian sorption is characterized by initially linear curves on a plot of reduced mass (Q_t/Q_∞, where Q_∞ is the total sorbed mass at the final equilibrium) versus the reduced time ($t^{1/2}/l$), which coincide for films of different thicknesses.

A series of workers [Mandelkern and Long (1951), Kokes, Long, and Hoard (1952), Drechsel, Hoard, and Long (1953), Long and Kokes (1953), and Park (1952 and 1953); see ref. 1] concluded that non-Fickian sorption processes were observed when a given polymer–penetrant mixture was studied at a temperature below the glass-transition point of the system. Non-Fickian diffusion is best studied in a series of successive interval absorption experiments. According to this experimental protocol, an initially dry film is subjected to a series of successive absorption runs covering relatively narrow vapor pressure intervals ($\Delta p = p_f - p_i$), with p_f for one run serving as p_i for the next one. Odani and coworkers[2–5] studied extensively a significant number of glassy-polymer/organic-vapor systems that exhibited non-Fickian kinetic behavior, and they observed a well-defined pattern in the Q_t/Q_∞–$t^{1/2}$ curves as p_i increased. The most complete form of this pattern, proposed by Fujita,[1] consists of the following steps:

S-shaped → Pseudo-Fickian → Two-stage
→ Pseudo-Fickian (or s-shaped) → Fickian

Correspondence to: V. Dimos (vdim@chem.demokritos.gr).
Contract grant sponsor: PLATO Bilateral S&T Cooperation Program (between Greece and France; funded by General Secretariat of Research and Technology (GSRT) Greece).
Contract grant sponsor: Excellence in the Research Institutes Program Action 3.3.4 (funded by GSRT-Greece and European Union (EU)).

They also reported several deviations from this pattern, which have also been observed in subsequent studies of other systems.[6–10] The standard feature of all studies is the transition to two-stage curves with rising p_i. Non-Fickian diffusion is also studied in integral sorption experiments, where p_i is 0 and p_f is comparatively large. In this case, S-shaped absorption curves are usually observed, and they initially lie below and then cross the corresponding desorption ones (convex upward).

Non-Fickian kinetic behavior is interpreted in terms of (1) the viscoelastic response of the glassy polymer to the osmotic stress induced by the penetrant[1,10–14] or (2) the longitudinal differential swelling stresses induced by (and closely following the buildup or decay of) the concentration gradients that develop across the film during the sorption process.[10,11,15,16] In reality, both mechanisms are expected to operate during a sorption experiment, but the former is most commonly adopted for the interpretation of anomalous kinetic behavior. Viscous relaxation is clearly manifested in two-stage sorption kinetics, in which the first stage corresponds to limited sorption and subsequent diffusion into the elastically swelling or unrelaxed polymer up to a quasi-equilibrium and the second stage is the result of long-range chain rearrangements, which permit further (delayed or viscous) swelling and are slow on the diffusion timescale. The rate of viscous relaxation (governed by the relaxation frequency, β, or reciprocal relaxation time, $\tau = 1/\beta$) with respect to that of the diffusion process (governed by D/l^2, where D is the diffusivity of the penetrant in the polymer) is expressed by the dimensionless parameter $\beta l^2/D$ (or by its reciprocal, the diffusion Deborah number $\tau D/l^2$). The condition $\beta l^2/D \rightarrow \infty$ or $\beta l^2/D \rightarrow 0$ results in Fickian diffusion within the purely relaxed or purely unrelaxed polymer matrix, respectively. The condition for a two-stage behavior, with well-separated first and second stages, is $\beta l^2/D < 1$. In this case, the relevant diffusion and the viscous relaxation processes can be studied independently of each another, under conditions of negligible differential swelling stresses, as a result of the absence of significant concentrations gradients. The results obtained by this type of analysis indicate that the behavior of β with the concentration is complex. Thus, the work of Fujita and coworkers[2–4] indicates that β is in general a function of the penetrant concentration (C) as well as the concentration interval of the sorption run (ΔC). On the other hand, two-stage sorption data of acetone, as well as methanol (MeOH), in cellulose acetate[7,8] have revealed a very weak dependence of β on C coupled with substantial dependence of β on ΔC. Moreover, the relevant data of the poly(methyl methacrylate) (PMMA)–methyl acetate system[3,9] indicate that β shows a very weak, if any, dependence on the concentration as long as the system remains in the glassy state, but it becomes increasingly concentration-dependent as the effective glass-transition temperature (T_g) of the polymer–penetrant system is approached.

S-shaped absorption curves are expected for values of $\beta l^2/D \approx 1$, a condition normally fulfilled in the case of integral experiments covering relatively large ΔC intervals. The S-shape of the Q_t–$t^{1/2}$ absorption curves obtained at the low-concentration end of a series of interval runs is usually attributed to a viscous relaxation process.[1,2,12] However, a systematic investigation of the acetone and MeOH vapors in cellulose acetate,[7,8] as well as the methyl acetate vapor in PMMA,[9] indicates that the curves are diffusion-controlled. It would be of particular interest to investigate the relevant behavior of other systems.

An extreme case of relaxation-controlled transport, associated with a sharp concentration profile, is case II kinetics, in which Q_t is linear when plotted on a t scale. Case II kinetics occur in absorption experiments characterized by (1) a sufficiently large difference of the penetrant solubility ($S = C/a$, where a is the penetrant activity) in the unrelaxed and fully relaxed polymers and (2) sufficiently large ΔC values to ensure steep changes in D and β. These conditions are expected to be fulfilled during absorption from the liquid phase. The most extensively studied case II system is liquid MeOH–PMMA at ambient and subambient temperatures (e.g., refs. 17–19). The steep concentration dependence of both D and β, required for the modeling of this system in terms of viscous relaxation effects, can be assessed experimentally in a series of interval vapor sorption experiments, as discussed previously.

In this work, an experimental study of the sorption kinetic behavior in the PMMA–MeOH vapor system at 25°C is presented. The system has been extensively studied with liquid MeOH,[17–19] but surprisingly, only limited data from the vapor phase exist.[20] The main features of non-Fickian kinetics are studied in a series of interval and integral absorption runs, with particular emphasis on (1) the investigation of the predominant transport mechanism in initially dry films with increasing vapor activity and (2) the kinetic analysis of two-stage curves to examine separately the diffusion and relaxation processes in the high-concentration region.

EXPERIMENTAL

PMMA powder, with an average molecular weight of 120,000, supplied by Aldrich (Steinein, Germany, code no. 18,223-0), was used to prepare the polymer membranes for the PMMA–MeOH system under investigation. Two membranes of different thicknesses (51 μm for M51 and 8 μm for M8) were investigated. M51 was prepared by the casting of a 20 wt % solution of PMMA in acetone (analytical-reagent-grade) onto a glass plate and leveling with a Gardner knife, whereas a 10 wt % solution was used for M8. Both membranes

were removed from the glass plate by immersion in distilled water.

To remove the residual acetone, M51 was evacuated for 4 days, and then the temperature was gradually raised (over a period of 24 h) up to 115°C and kept constant for a period of 2 h. Finally, the membrane was gradually cooled to room temperature. T_g of M51, after the treatment, was found to be 117°C, whereas it was proved to be totally amorphous. Because of the fragility of the M8 membrane, it was not possible to repeat the same procedure for the removal of the residual acetone. Hence, M8 was kept *in vacuo* for a period of 40 days, and then the temperature was raised to 50°C, *in vacuo*, for another 10 days. T_g was determined to be 119°C, whereas a second analysis of the same sample resulted in the same T_g, which indicated the total removal of acetone. M8 was also found to be totally amorphous.

Sorption experiments were carried out in a vacuum apparatus, with an MK2-M5 CI electronics microbalance (Churchfields, UK), with a sensitivity of 0.1 μg, and an accuracy of 1 μg. The balance operation capabilities extended from vacuum to 20 atm and over a wide range of temperatures (10–80°C). Sample and counterweight jacketed tubes were used, both thermostated at the desired temperature, whereas the temperature reading was acquired from within the sample tube via a K thermocouple. The apparatus feeding system consisted of a temperature-controlled liquid MeOH flask, which was connected to a 6-lt ballast tank, to avoid a significant pressure drop during the pressure step change. A valve was installed between the feeding system and the balance inlet. The aforementioned apparatus was installed within a temperature-controlled chamber, which operated between 20 and 40°C. The drift of the balance during a blank experiment with an atmosphere of MeOH was found to be 2.25×10^{-5} μg/s (<0.2 μg/48 h), whereas the standard deviation of a statistical sample of 26,069 measurements was found to be 31 μg.

The studied polymer membrane sample and a counterweight of similar mass were suspended from the corresponding balance phalanx, and the apparatus was evacuated for 5 days. During this time, sorbed air and traces of acetone were removed from the sample, and this resulted in a constant measured mass. For subsequent sorption experiments, the feeding lines were disconnected from the balance, and the temperature of the liquid penetrant (vapor source) was set to the appropriate value to create the desired vapor pressure (p_f). When the pressure reached the equilibrium value, the ballast tank was connected to the balance ($t = 0$). The mass uptake of the sample was recorded by a computer, with a sampling time of 2–12 s, which depended on the diffusion rate. After equilibrium was achieved, the balance was disconnected from the feeding lines, and a new experiment was initiated by raising the temperature of the MeOH source to a higher value to obtain a next step of a given interval series or by evacuation before a new series of interval sorption curves or a new integral experiment.

The pressure step changes in a typical series of interval absorption curves (e.g., series S1, S5, and S6 of this study) are kept small enough so that the mass gain of the membrane, due to penetrant absorption, does not exceed 2% of the dry polymer mass. In that case, diffusivity may be assumed to be constant during the sorption run, and the value of the diffusion coefficient may be calculated for the corresponding range of concentration increments caused by the solution of the penetrant. Furthermore, small step changes of the pressure in each experiment result in a negligible raise (drop) of the penetrant atmosphere density, and this ensures that the buoyancy difference is negligible and the measured mass change corresponds to the mass change of the film due to penetrant sorption.

The construction of a typical sorption curve requires plotting the reduced mass gain (i.e., Q_t/Q_∞) of the film versus the square root of time ($t^{1/2}$) or reduced time ($t^{1/2}/l$). The parameters that can be deduced from a two-stage sorption experiment are Q_∞, the quasi-equilibrium value (Q_q; i.e., the sorbed mass at the end of the first stage), D (which controls the first stage), and β (which controls the second stage).

The dry sample M8 used in this sorption study consisted of four rectangular membranes of PMMA, each 1.5 cm × 9 cm, with a total weight of 56.4 mg. The sample M51 was one rectangular (1.5 cm × 7.5 cm) membrane of PMMA that weighed 62.1 mg. Both samples could be assumed to be infinite surface media for one-dimensional molecular diffusion studies as the ratio of thickness to the smaller surface dimension was equal to or less than 0.0034. Analytical reagent MeOH was used as the vapor source. The experiments were carried out at 25°C and at vapor pressures varying from 14 to 122 Torr. The chamber temperature was set 10°C above the experimental temperature to ensure that no vapor condensation would occur in the feeding system. The MeOH saturation pressure was calculated to be 127.94 Torr at 25°C.[21]

RESULTS AND DISCUSSION

Sorption isotherm

Membrane M8, which was most extensively studied, was initially subjected to three series of interval sorption runs (S1–S3). The vapor pressure in all three interval series varied in the range of 0–120 Torr, but the size of Δp ($p_f - p_i$) and hence ΔC ($C_f - C_i$, where C_f is the final concentration and C_i is the initial concentration) of each run increased from one series to the next. Subsequently, M8 was subjected to a series of integral runs (S4), with $p_i = 0$ ($C_i = 0$) in all runs, but

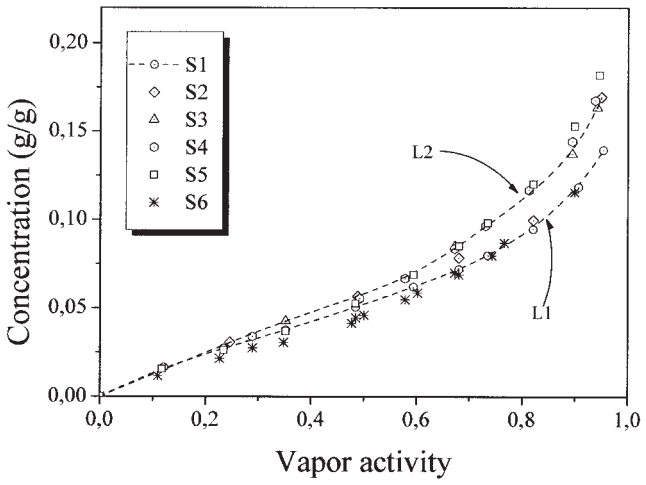

Figure 1 Sorption isotherms of MeOH in PMMA at 25°C, including data from series S1–S5 in M8 and series S6 and S7 in M51. Dashed lines L1 and L2 have been drawn through the data of series S1 and S2–S5, respectively.

different p_f (and hence $\Delta C = C_f$) values. Finally, a fifth series (S5) with pressure steps similar to those of S1 was performed to check the effect of the previous sorption history on the sorption kinetic behavior. The effect of thickness was also studied in selected interval (series S6) and integral experiments (series S7) in the thicker M51 membrane.

The sorption isotherms of MeOH in PMMA, deduced from the apparent equilibrium concentrations of series S1–S7, are displayed in Figure 1. Similar to previously reported results for the same system,[20] the sorption isotherms of this system increased sharply at high vapor activity, this being typical of Flory–Huggins solution behavior, whereas it appears to be concave to the activity axis at a low MeOH pressure, this indicating the sorption of MeOH vapor in the fixed microcavities, which constitute the excess free volume of the glassy PMMA membrane (dual-mode sorption).[20] The equilibrium data obtained from the series S2–S5 fall on the same line (Fig. 1, dashed line L2), which displays a shift to higher concentration values in comparison with the line deduced from series S1 equilibrium data (Fig. 1, dashed line L1). This shift probably reflects the annealing of the membrane caused by the upholding of the polymer film at high MeOH concentration values for a long period of time during the first series of absorption runs. Furthermore, the Flory–Huggins interaction parameter, deduced from the high-activity data of series S1, is 1.285, whereas the one calculated from the high-activity data of series S5 is shifted to 1.144, a value close enough to 1.1, which is the one deduced from liquid ($a = 1$) penetration experiments in the same system at 24°C.[18] Therefore, it can be assumed that L2 represents the final sorption isotherm of the MeOH–PMMA system. The discrepancy between lines L1 and L2 (Fig. 1) tends to diminish at the low-concentration end (in the region of the excess free-volume filling).

The experimental sorption isotherm for M51 concurs with the one of the S1 series (L1), with the exception of the low-activity region (referring to excess free-volume filling), where a lower amount of excess free volume in M51, in comparison with M8, is indicated, probably because of the different preparation and treatment procedures followed for the two samples.

Interval sorption experiments

Series S1 of interval absorption runs in M8 consists of 10 successive runs (Fig. 2). In contrast to the findings in most studied systems,[1–9] the first step of S1 displays a nearly Fickian character rather than an S-shaped one. With increasing p_i, the nonlinear late-time portion of the kinetic plots (1) becomes more protracted and (2) constitutes an increasingly larger part of the overall curve. As a result, there is a progressive shift from clearly pseudo-Fickian behavior [S1(2) and S1(3)] to two-stage behavior, with well-separated first and second stages [S1(6) to S1(10)]. The contribution of the first stage to the overall sorption process decreases with increasing activity of MeOH vapor, in accordance with previous studies.[7–9] In the case of two-stage curves, the rate of the first stage increases with p_i (C_i), as expected for a diffusion-controlled process with a concentration-dependent D. On the other hand, the progressive shift to Fickian behavior found for other systems at high concentrations,[1–6] as a result of a steep increase of the relaxation rate with increasing pressure, was not observed in this study, and this indicates that even at the higher concentration reached the polymer–penetrant mixture is well below its T_g.

The effect of the membrane thickness was studied with a series of seven successive absorption runs (S6), with Δp intervals similar to those of S1, on a thicker PMMA membrane (M51). The kinetic pattern followed in S6 is identical to the one followed in S1 (Fig. 2). A comparison of the first runs of both membranes [S1(1) and S6(1)], on a plot of the reduced mass versus the reduced time ($t^{1/2}/l$), indicates that it is predominantly diffusion-controlled because there is only a small discrepancy between the two curves (Fig. 2). In the following three runs, sorption in M51 exhibits a better resemblance to Fickian behavior than sorption in M8. This illustrates the slower diffusion rate (D/l^2) governing sorption in thicker membranes, which allows macromolecular relaxation to occur during the diffusion-controlled first stage, in accordance with the fact that the Deborah number for a thick membrane of a given polymer is lower than the Deborah number of a thinner one, even if D and β remain the same in both cases ($D/\beta l_1^2 < D/\beta l_2^2$ if $l_1 > l_2$). The progressive separation of diffusion and relaxation processes, as C_i

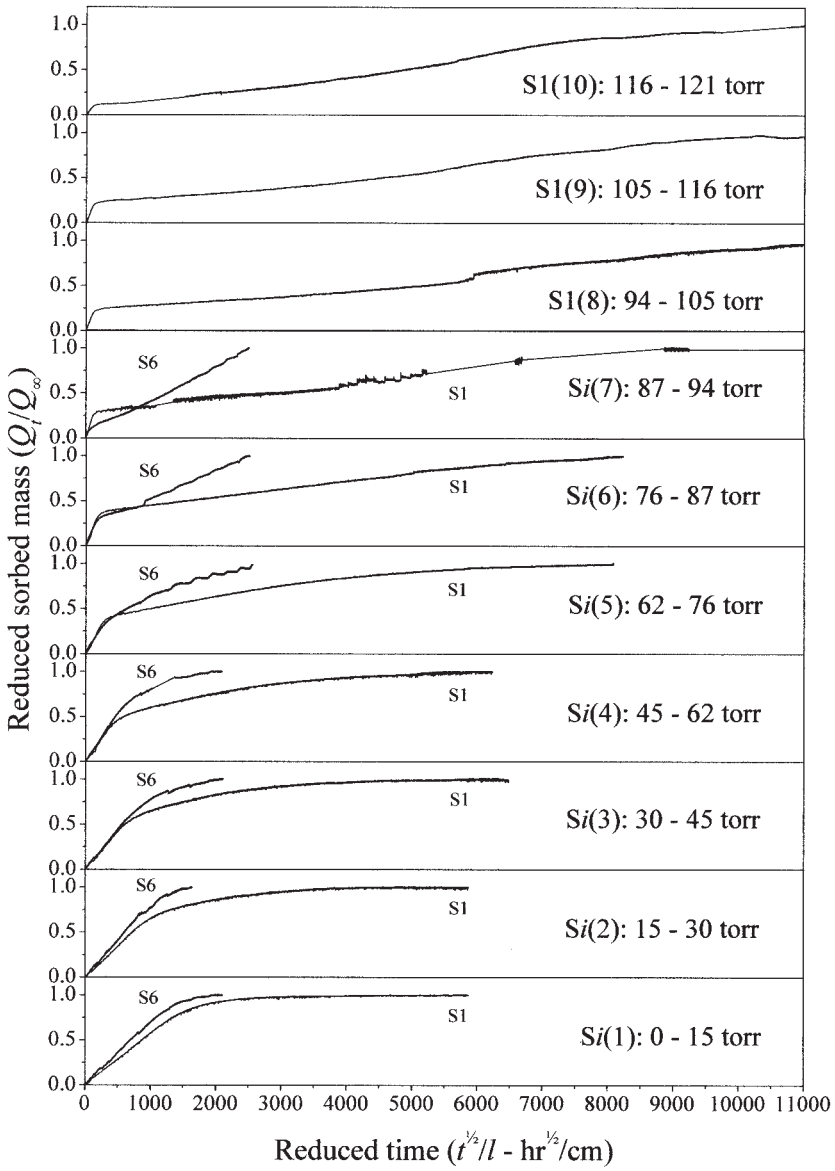

Figure 2 Comparison of successive absorption kinetic runs of MeOH in amorphous PMMA films of 8 μm (S1) and 51 μm (S6) at 25°C. C_f (g/g) was 0.016 [S1(1)], 0.027 [S1(2)], 0.038 [S1(3)], 0.05 [S1(4)], 0.062 [S1(5)], 0.072 [S1(6)], 0.08 [S1(7)], 0.095 [S1(8)], 0.119 [S1(9)], and 0.14 [S1(10)].

increases, is clearly demonstrated by the corresponding coincidence of M8 and M51 curves at the initially linear diffusion-controlled part of the sorption curves and their departure from each other on the late-time relaxation-controlled stage (Fig. 2).

The effect of increasingly higher ΔC of sorption runs is shown in the plots of series S2 (Fig. 3) and S3 (Fig. 4) in M8. Both series follow the pattern established in S1, with the exception of the first run, which exhibits an indiscernible S-shape in S2 and a distinct one in S3. Furthermore, the rate of the second stage of two-stage curves increases with ΔC, and this results in less well separated two-stage curves. This is best illustrated by a comparison of curves S3(3), S2(4), and S1(8) (Fig. 5), which correspond to approximately the same C_i value ($\sim$0.08 g/g) to different ΔC values (0.052, 0.021, and 0.015 g/g, respectively). It is apparent that the diffusion-controlled stage concurs in all three curves, whereas the relaxation-controlled stage becomes faster with increasing ΔC.

Because of the difference of the sorption isotherm between S1 and subsequent series S2–S4 (Fig. 1), M8 was resubjected to a fifth series of successive absorption runs (S5), with pressure steps similar to those of S1 (Fig. 6). Series S5 exhibited close similarity, both in shape and in rate, with series S1, and this indicated that the observed shift in the isotherm did not affect the main futures of the system's sorption kinetic behavior. Furthermore, the equilibrium concentration data of the S5 series are in good agreement with line

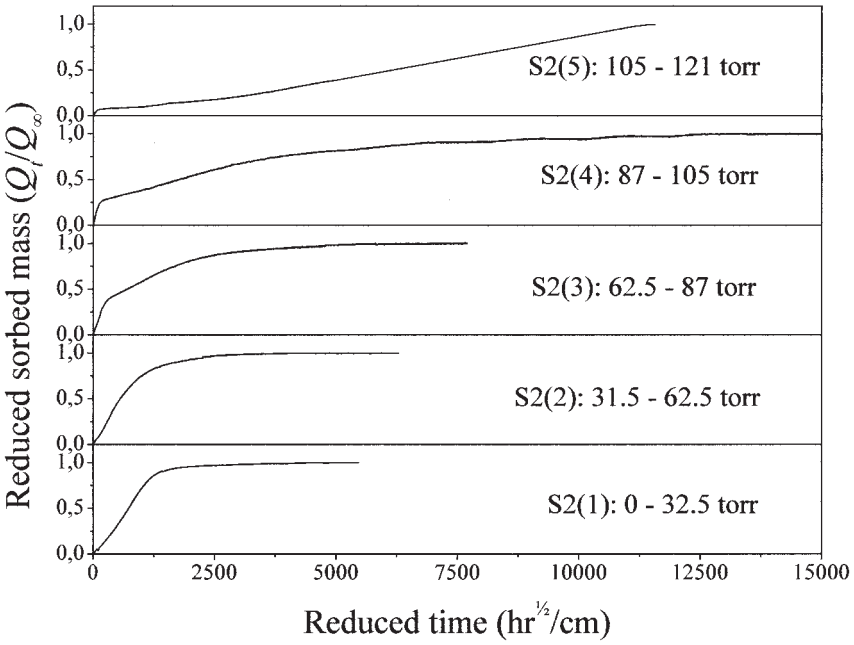

Figure 3 Series S2 of successive absorption kinetic runs of MeOH in amorphous, 8 μm PMMA film at 25°C. C_f (g/g) was 0.031 [S2(1)], 0.057 [S2(2)], 0.078 [S2(3)], 0.1 [S2(4)], and 0.169 [S2(5)].

L2 (Fig. 1), and this indicates that the sorption isotherm shift cannot be attributed to the higher ΔC values of series S2–S4; therefore, L2 represents the system's final isotherm.

Integral sorption experiments

The effect of ΔC for experiments with $C_i = 0$ was further studied in series S4 and S7 of integral absorption runs in M8 and M51, respectively. A comparison is again made via plotting on a $t^{1/2}/l$ scale (Fig. 7). Because of the difference between the sorption isotherms of M8 (Fig. 1, line L2) and M59 (Fig. 1, line L1), the compared absorption curves of the two membranes are chosen to refer to the same ΔC value ($\sim C_f$), which does not necessarily correspond to the same Δp value (p_f). As already mentioned, for the lowest ΔC value studied (Figs. 2 and 7), the Fickian shape of the absorption curves indicates that the process is predominantly diffusion-controlled, although there is a slight thickness effect. Deviation from Fickian kinetics increases with rising ΔC (Fig. 7), as evidenced by (1) a progressively more intense S-shape of the absorption curves and (2) a more pronounced thickness effect, with respect to C_f. Furthermore, one may observe that the inflection point, as well as the equilibrium estab-

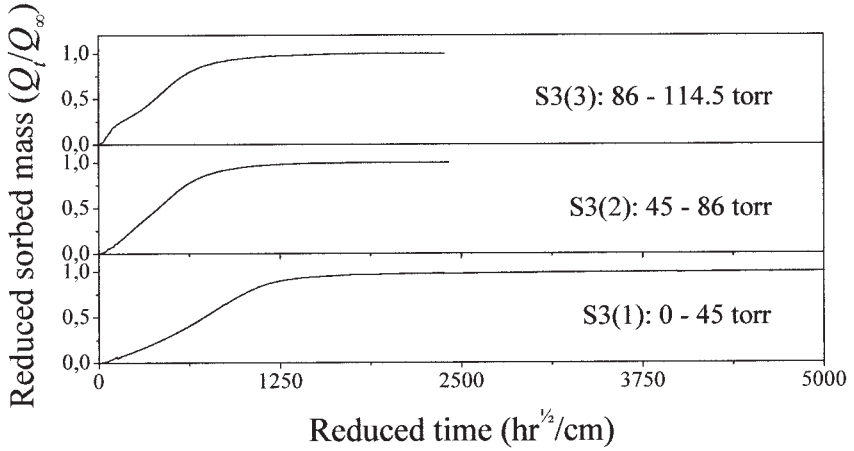

Figure 4 Series S3 of successive absorption kinetic runs of MeOH in amorphous, 8 μm PMMA film at 25°C. C_f (g/g) was 0.043 [S3(1)], 0.085 [S3(2)], and 0.137 [S3(3)].

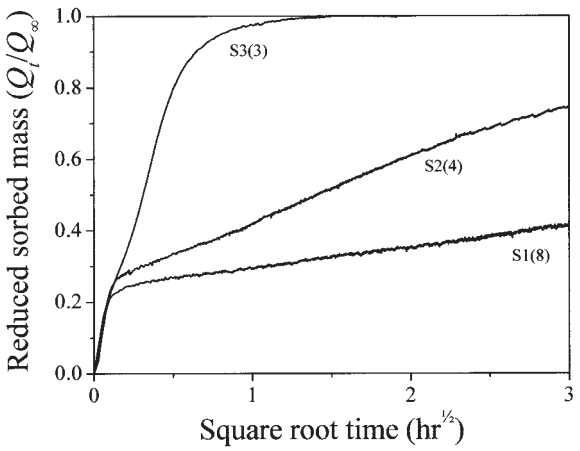

Figure 5 Comparison of two-stage absorption curves with approximately the same C_i values (~0.08 g/g) but with different ΔC values (g/g) of 0.015 [S1(8)], 0.021 [S2(4)], and 0.052 [S3(3)].

lishment, moves to shorter times as the concentration difference rises. A simple power law is often used to quantify deviations from Fickian behavior:[10]

$$Q_t/Q_\infty = kt^n \tag{1}$$

where n has a value of 0.5 for Fickian kinetics under semi-infinite conditions. Increasing values of n (>0.5) denote increasing deviations from Fickian kinetics. A value of $n = 1$ corresponds to case II sorption, exhibiting an extreme form of relaxation-controlled kinetics. For S4, the values of n deduced from the slopes of the relevant ln–ln plots (Fig. 8) indicate a gradual conversion from Fickian kinetics at low ΔC to case II kinetic behavior in the higher ΔC regime. At the maximum activity of MeOH vapor ($a = 0.95 - p_f = 120$ Torr) attained in this study, the system exhibits nearly case II kinetics ($n \approx 1$). The observed approach to case II kinetics (Fig. 8, $p_f = 104$, 114, and 120 Torr) at the upper activity end is quite reasonable because it is well established that the sorption of liquid MeOH ($a = 1$) in initially dry PMMA films, at ambient temperatures, follows case II kinetics.[17–19]

Diffusion coefficient

Constant values of the diffusion coefficient in a polymer-fixed frame of reference (D_p) are calculated from the first stage of the two-stage absorption curves with the short-time approximation of the diffusion equation:[22]

$$Q_t/Q_\infty = 4(D_p t/\pi l^2)^{1/2} \tag{2}$$

The value of Q_q (the amount of the penetrant sorbed at the quasi-equilibrium) was estimated according to the following method proposed by Park.[23] A first approximate estimation of Q_q was used to calculate a value of D_p [eq. (2)] from the initially linear part of the Q_t/Q_q–$t^{1/2}$ plot. The calculated D_p value was used to construct the theoretical Fickian curve, in the range of $0.6 < Q_t/Q_q < 1$, according to the late-time approximation of the diffusion equation:[22]

$$Q_t/Q_\infty = 1 - \frac{8}{\pi^2}\exp(-D_p\pi^2 t/l^2) \tag{3}$$

The value of Q_q was iteratively reduced until the maximum D_p value was found, which produced a theoretical curve that does not cross the experimental one. D_p values were also calculated, according to the same procedure, from pseudo-Fickian curves (Fig. 9). The aforementioned criterion for the estimation of Q_q (and consequently D_p), though physically meaningful, is not necessarily very certain, especially in the case of not well separated first- and second-stage curves.

The diffusion coefficient was evaluated from all the kinetic curves of the S1, S5, and S6 series and from most of the pseudo-Fickian and two-stage curves of the S2 and S3 series, where the initial portion of the curve is linear and the concentration difference from the initial value to the pseudo-equilibrium value is small enough to assume a constant diffusion coefficient in the studied range. It is apparent that diffusivity increases with respect to the concentration (Fig. 10). Interestingly, the D_p values deduced at low concentrations (i.e., up to $C_f \approx 0.07$ g/g) tend to be more reproducible than those of the high-concentration regime.

According to the free-volume theory of Vrentas and Duda, the concentration dependence of the self-diffusion coefficient (D^*) is given by[24]

$$D^* = D_{01}\exp\left[-\frac{\gamma(\omega_1\hat{V}_1^* + \omega_2\xi\hat{V}_2^*)}{\hat{V}_f}\right]$$

$$\frac{\hat{V}_f}{\gamma} = \omega_1\left(\frac{k_{11}}{\gamma}\right)(k_{21} - T_{g1} + T) + \omega_2\left(\frac{k_{12}}{\gamma}\right)(k_{22} - T_{g2} + T) \tag{4}$$

where D_{01} is an adjustable pre-exponential factor; γ is the free-volume overlap factor; ω_1 and ω_2 represent the weight fractions of the penetrant and the polymer, respectively; $\hat{V}_1^*$ and $\hat{V}_2^*$ are the specific critical local free volumes required for a penetrant molecule jump and for a polymer jumping unit displacement, respectively; $\hat{V}_f$ is the specific average free volume of the mixture; and ξ is the ratio of the penetrant and polymer critical molar volumes. T_{g1} and T_{g2} are the glass-transition temperatures of the penetrant and polymer, respectively; and k_{11}, k_{12}, k_{21}, and k_{22} are related to the Williams–Landel–Ferry constants of the two components. D_p is related to D^* as follows:

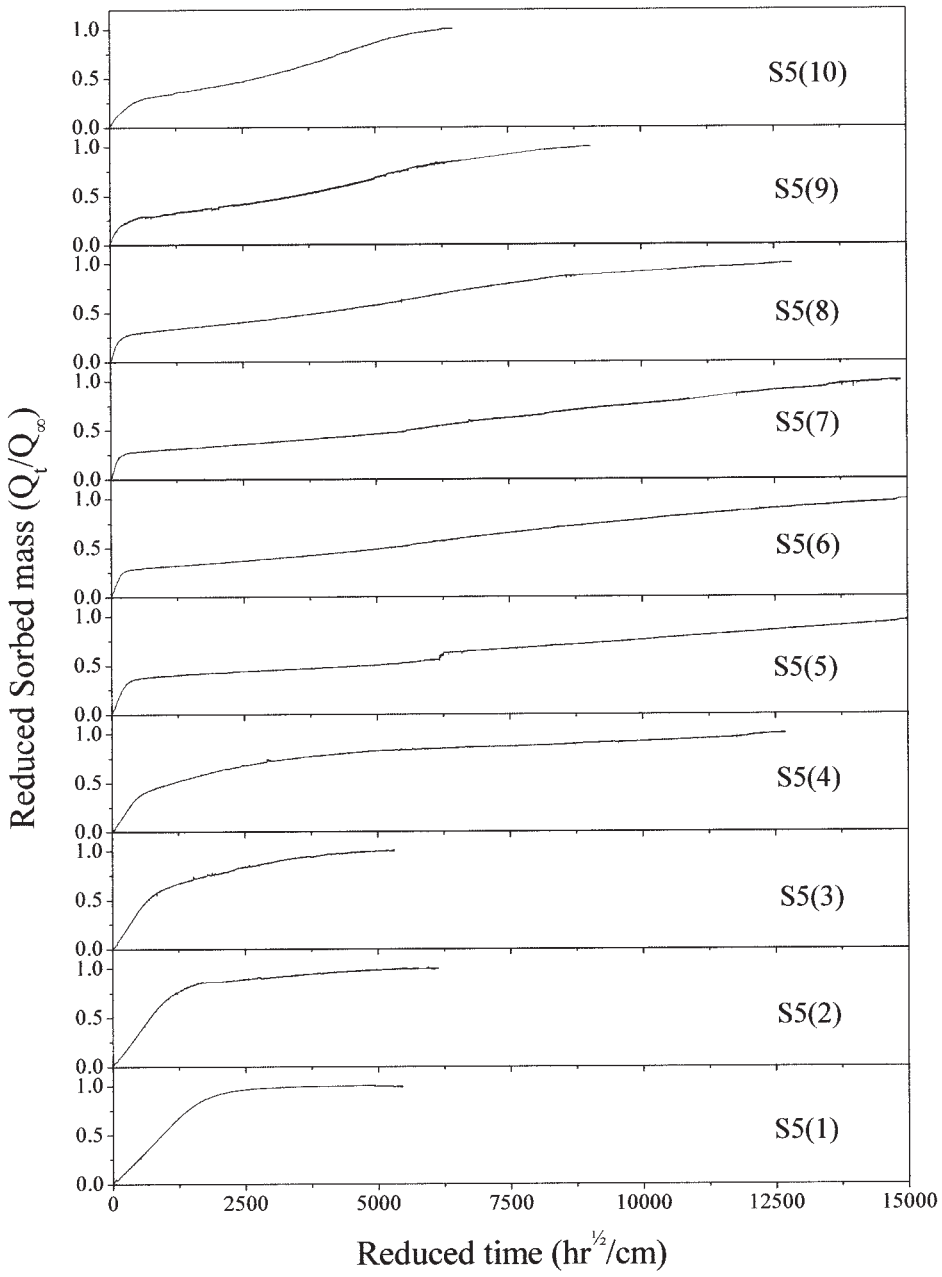

Figure 6 Series S5 of successive absorption kinetic runs of MeOH in amorphous, 8-μm PMMA film at 25°C. C_f (g/g) was 0.016 [S5(1)], 0.026 [S5(2)], 0.037 [S5(3)], 0.053 [S5(4)], 0.069 [S5(5)], 0.085 [S5(6)], 0.098 [S5(7)], 0.120 [S5(8)], 0.153 [S5(9)], and 0.188 [S5(10)].

$$D_p = D^*(1 - \varphi_1)^3 \frac{\partial \ln a}{\partial \ln \varphi_1} \tag{5}$$

where ϕ_1 is the penetrant volume fraction. Equation (4) strictly holds for polymer–penetrant systems above T_g, but it has been found to represent reasonably well the concentration dependence of the diffusivity of glassy systems relatively close to T_g.[9,25] It is interesting to identify up to what extent eq. (4) is applicable to the experimentally calculated D_p's (Fig. 10). Theoretical values of D_p, at 25°C were calculated by the application of eqs. (4) and (5) with $k_{11}/\gamma = 1.17 \times 10^{-3}$ cm^3/g K, $k_{21} - T_{g1} = -47.9$ K, $\hat{V}_1^* = 0.963$ cm^3/g,[26] $\xi = 0.0675$,[18] $k_{12}/\gamma = 3.05 \times 10^{-4}$ cm^3/g K, $k_{22} = 80$ K, $\hat{V}_2^* = 0.788$ cm^3/g,[27] and $T_{g2} = 388$ K (as an average T_g calculated for the studied sample). The activity versus the volume fraction derivative [eq. (5)] was estimated from the experimentally determined sorption isotherm (Fig. 1, line L2), whereas D_{01} was found to be 2.5×10^{-6} cm^2/s. It is apparent that the experimentally observed concentration dependence of the diffusivity is reasonably reproduced by the theoretically calculated diffusivity

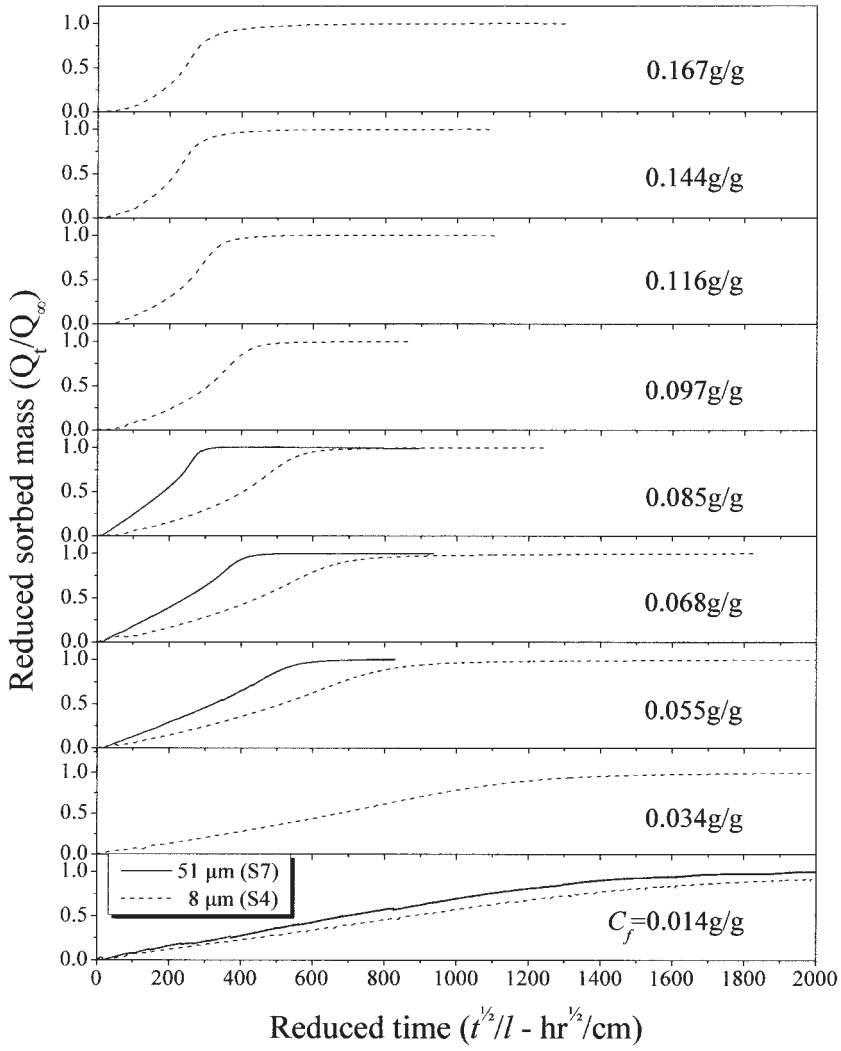

Figure 7 Comparison of the integral absorption kinetic runs (series S4 and S7) of MeOH in PMMA films of two different thicknesses at 25°C. C_i was 0 for all the experiments.

curve (Fig. 10, dashed line) for the studied concentration range higher than ~0.05 g/g; whereas below this value, the experimentally observed concentration dependence of D_p is less steep than the theoretically predicted one, as expected from the application of free-volume theory for the glassy state.[28]

Relaxation rate

When the first and second stages of a two-stage sorption curve are in good separation, it may be assumed that the second stage represents pure relaxation kinetics. One may calculate β by applying the integrated form of the first-order relaxation kinetic law, represented by eq. (6), with the assumption that β is constant:[9]

$$1 - Q_t/Q_\infty = (1 - Q_q/Q_\infty)\exp(-\beta t) \qquad (6)$$

On the basis of eq. (6), β is represented by the gradient of the second-stage experimental data, in a plot of $\ln(1 - Q_t/Q_\infty)$ versus t. Because in this system β is a function of both C and ΔC, for the estimation of the concentration dependence of β, values of the relaxation rate were calculated [eq. (6)] from two-stage curves covering relatively small ΔC regions. The relevant $\ln(1 - Q_t/Q_\infty)$–t plots exhibit reasonable conformity to eq. (6) for considerable time periods, but deviations were observed at longer times. Accordingly, β values were estimated from the initially linear parts of these plots. Although there are discrepancies between the results obtained from different sorption series, the calculated β values clearly indicate that for the studied system β is an increasing function of C (Fig. 11). Comparing the relative increase of the diffusivity and the relaxation rate values in the concentration range of two-stage behavior, we find that the concentration

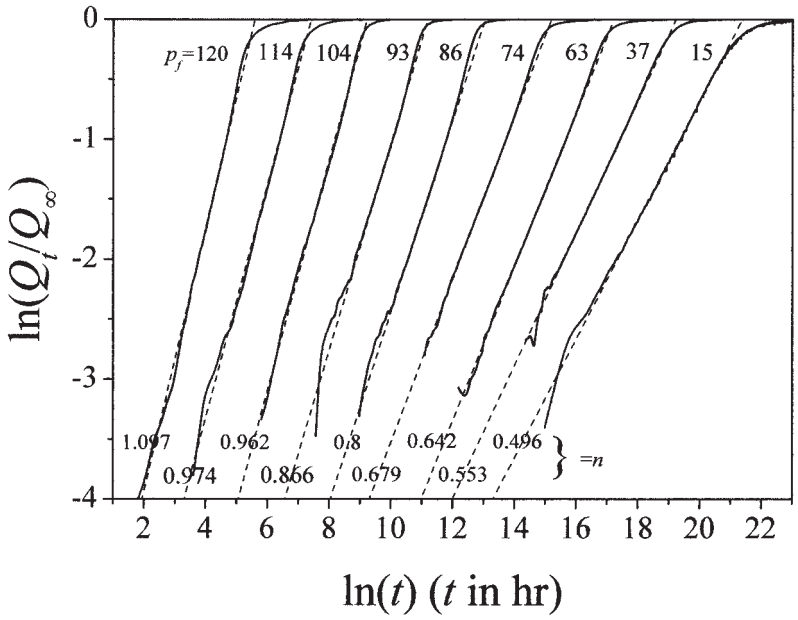

Figure 8 Integral absorption kinetics (S4) of MeOH in amorphous, 8-μm PMMA film at 25°C plotted on an ln–ln scale. p_f (Torr) of each experiment and the exponent n [eq. (1)] deduced from the slope of each curve are indicated in the upper and lower parts of the plot, respectively. The curves have been displaced laterally on the ln t scale for the sake of clarity by an addend of $k = 0$ ($p_f = 120$), 2 ($p_f = 114$), 3.5 ($p_f = 104$), 5 ($p_f = 93$), 6.2 ($p_f = 86$), 8 ($p_f = 74$), 9.7 ($p_f = 63$), 11 ($p_f = 37$), or 12.5 ($p_f = 15$).

dependence of D_p is much stronger than the one presented by β values. For example, in the concentration range between 0.06 and 0.10 g/g, diffusivity increases nearly one order of magnitude, whereas the relaxation rate increases only by a factor of ~3.

The D_p and β values (Figs. 10 and 11, respectively) obtained from the two-stage experiments were used to calculate the corresponding $\beta l^2/D$ parameter. Two-stage curves with well-separated stages [e.g., curves S1(7)–S1(10), Fig. 2] are characterized by values of $\beta l^2/D$ of the order of 10^{-3} ($\ll 1$). On the other hand, the gradual merging of the two stages as ΔC increases (Fig. 5) is reflected in the increase of $\beta l^2/D$ from the value of 0.0012 for the S1(8) run to the value of 0.0020 for S2(4). The profound merging of the two stages in the case of the S3(3) run prevents the calculation of the relaxation rate parameter with the aforementioned method.

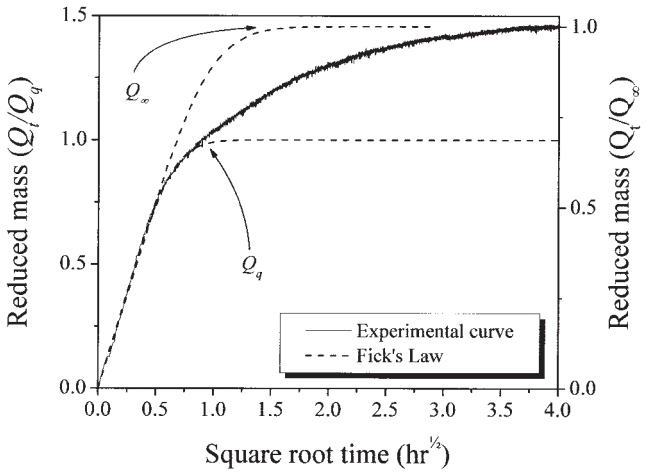

Figure 9 Calculation procedure for the estimation of Q_q and D_p in the case of a pseudo-Fickian curve (see the text).

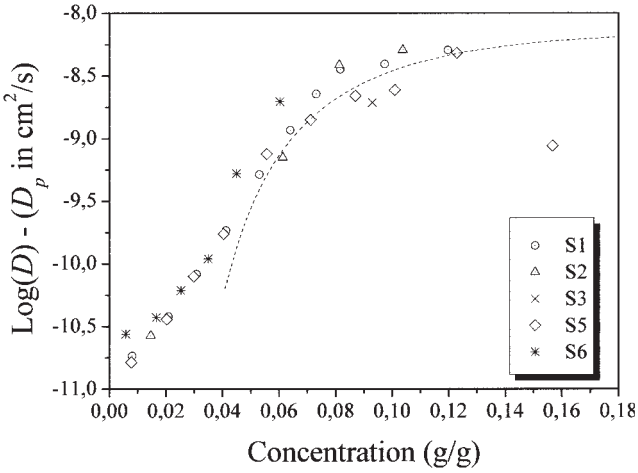

Figure 10 Concentration dependence of D_p of MeOH in amorphous PMMA for series S1–S5 in M8 and for series S6 in M51. The calculated D_p values were assumed to correspond to the mean concentration of the first stage, where C_q is the concentration at the pseudo-equilibrium: $C_{mean} = C_i + 0.5(C_q - C_i)$. The dashed line represents the diffusivity isotherm calculated by the Vrentas–Duda free-volume theory [eqs. (4) and (5)].

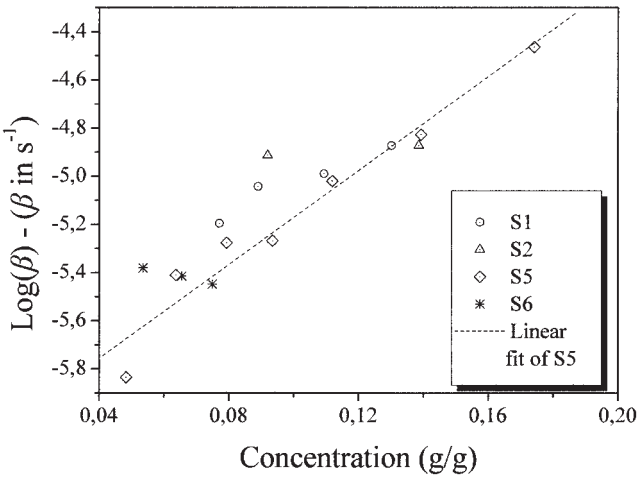

Figure 11 Concentration dependence of β for the amorphous PMMA–MeOH system at 25°C deduced from the second stage of two-stage curves of series S1–S3 and S5 in M8 and series S6 in M51. The calculated β values were assumed to correspond to the mean concentration of the second stage: $C_{mean} = C_f - 0.5(C_f - C_q)$. The dashed line represents a linear regression of the S5 series data.

CONCLUSIONS

The sorption isotherm of the chosen system, in line with previous studies,[20] exhibits initially the convex-upward curvature that characterizes micromolecular sorption in the excess free volume of the polymer matrix. The equilibrium data obtained from different sorption series in M8 indicate that this part of the isotherm is quite reproducible for both the as-received and annealed polymers. At higher activities, the sorption isotherm concaves upward, this being typical of Flory–Huggins sorption behavior. In this region, differences in the equilibrium uptake from the S1 series (as-received PMMA) to the final system isotherm (S2–S5) appear as a result of the polymer annealing. These differences in equilibrium sorption do not materially affect the overall kinetic behavior of the system. The lower Flory–Huggins parameter value presented by the L2 isotherm (series S2–S5), compared with the S1 one, represents the aforementioned annealing.

The kinetic pattern followed in the series of interval runs with relatively small ΔC values (series S1 and S5 in M8 and series S6 in M51) shows a progressive shift from Fickian behavior to pseudo-Fickian behavior and finally to two-stage behavior with increasing C_i. The shift from pseudo-Fickian kinetics to two-stage kinetics occurs at concentrations higher than the ones corresponding to the free-volume-filling region of the sorption isotherm, and this indicates that the relaxation mechanism becomes significant when the excess free volume of the polymer matrix is filled with penetrant molecules. This is also in line with the fact that considerable discrepancies between the initial (as-received polymer) and final (annealed polymer) sorption isotherms of M8 occur mainly at concentrations exceeding those of the excess free-volume-filling region. A comparison of the corresponding two-stage kinetic curves at high concentration with respect to C_i and ΔC, for membranes of different thicknesses, on a reduced timescale verifies the diffusion- and relaxation-controlled nature of the first and second stages, respectively.

The system's behavior in experiments with $C_i = 0$ and increasingly higher ΔC values indicates that for sufficiently small ΔC values, the sorption process is predominantly diffusion-controlled and then relaxation-controlled, as shown by the shape of the relevant Q_t/Q_∞–$t^{1/2}/l$ plots, the negligible discrepancies between membranes of different thicknesses, and the value of n [eq. (1)], which tends to 0.5 at the lowest studied p_f value (15 Torr). The same conclusion regarding the predominant rate-determining process at low concentrations has been drawn for other glassy-polymer/organic-vapor systems.[7–9] With increasing ΔC, the intensification of the S-shape shown by the relevant kinetic plots and the increasing discrepancy between M8 and M51 kinetics indicate that the viscous relaxation effects become important. Eventually, as shown by kinetic analysis of the M8 data at the high-concentration end on the basis of a power law [eq. (1)], the sorption process becomes purely relaxation-controlled, in line with the well-established case II sorption of liquid MeOH in PMMA, at ambient temperatures.[17–19]

Two-stage curves with well-separated first and second stages were analyzed to deduce the concentration dependence of the diffusion and relaxation processes. The concentration dependence of D_p, deduced from the first stage of these curves, shows reasonably good conformity with the free-volume theory of Vrentas and Duda, which is strictly applicable to the rubbery state. The relaxation rate values deduced from the second stage were also found to be an increasing function of C. On the other hand, a quantitative comparison of the rate of the second stage in the case of two-stage curves referring to the same C_i value but different ΔC values indicates a much stronger dependence of β on ΔC.

The application of Park's method in the case of pseudo-Fickian kinetics results in reproducible D_p values, which indicate the validity of the method for pseudo-Fickian curves. The deviation of the deduced D_p values from the free-volume theory of Vrentas and Duda is in line with previous reports.[28]

References

1. Fujita, H. Adv Polym Sci 1961, 3, 1.
2. Fujita, H.; Kishimoto, A.; Odani, H. Prog Theor Phys Suppl (Kyoto) 1959, 10, 210.
3. Kishimoto, A.; Fujita, H.; Odani, H.; Kurata, M.; Tamura, M. J Phys Chem 1960, 64, 594.
4. Odani, H.; Kuda, S.; Kurata, M.; Tamura, M. Bull Chem Soc Jpn 1961, 37, 571.

5. Odani, H.; Kuda, S.; Tamura, M. Bull Chem Soc Jpn 1966, 39, 2378.
6. Billovits, G. F.; Durning, C. J. Macromolecules 1993, 26, 6927.
7. Sanopoulou, M.; Roussis, P. P.; Petropoulos, J. H. J Polym Sci Part B: Polym Phys 1995, 33, 993.
8. Sanopoulou, M.; Petropoulos, J. H. Polymer 1997, 38, 5761.
9. Boom, J. P.; Sanopoulou, M. Polymer 2000, 41, 8641.
10. Sanopoulou, M.; Petropoulos, J. H. Macromolecules 2001, 34, 1400.
11. Crank, J. J Polym Sci 1953, 11, 151.
12. Durning, C. J. J Polym Sci Polym Phys Ed 1985, 23, 1831.
13. Petropoulos, J. H. J Polym Sci Polym Phys Ed 1984, 22, 1885.
14. Thomas, N. L.; Windle, A. H. Polymer 1982, 23, 529.
15. Petropoulos, J. H.; Roussis, P. P. J Membr Sci 1978, 3, 343.
16. Samus, M. A.; Rossi, G. Macromolecules 1996, 29, 2275.
17. Thomas, N. L.; Windle, A. H. Polymer 1978, 19, 255.
18. Durning, C. J.; Hassan, M. M.; Tong, H. M.; Lee, K. W. Macromolecules 1995, 28, 4234.
19. Stamatialis, D. F.; Sanopoulou, M.; Petropoulos, J. H. Macromolecules 2002, 35, 1021.
20. Connelly, R. W.; McCoy, N. R.; Koros, W. J.; Hopfenberg, H. B.; Stewart, M. E. J Appl Polym Sci 1987, 34, 703.
21. Perry, R. H.; Green, D. W. Perry's Chemical Engineers' Handbook, 7th ed.; McGraw-Hill: New York, 1999.
22. Crank, J. The Mathematics of Diffusion, 2nd ed.; Clarendon: Oxford, 1976.
23. Park, G. S. Trans Faraday Soc 1961, 57, 2314.
24. Vrentas, J. S.; Duda, J. L. J Polym Sci Polym Phys Ed 1977, 15, 417.
25. Dubreuil, A. C.; Doumenc, F.; Guerrier, B.; Allain, C. Macromolecules 2003, 36, 5157.
26. Hassan, M. M.; Durning, C. J. J Polym Sci Part B: Polym Phys 1999, 37, 3159.
27. Zielinski, J. M.; Duda, J. L. AIChE J 1992, 38, 405.
28. Billovits, G. F.; Durning, C. J. Macromolecules 1994, 27, 7630.